Available online at www.sciencedirect.com
SCIENCE DIRECT®
Journal of Photochemistry and Photobiology A: Chemistry 163 (2004) 135–140
Journal of Photochemistry and Photobiology A:Chemistry
www.elsevier.com/locate/jphotochem

# Viscosity effects on 9,10-dicyanoanthracene-sensitized photooxidation of *N*,*N*-dibenzylhydroxylamine and its derivatives in protic polar solvents

Kohsuke Ushirokawa [a], Takashi Koike [a], Kenta Tanaka [b], Tetsutaro Igarashi [a], Tadamitsu Sakurai [a,*]

[a] *Department of Applied Chemistry, Faculty of Engineering, Kanagawa University, Kanagawa-ku, Yokohama 221-8686, Japan*
[b] *High-Tech Research Center, Kanagawa University, Kanagawa-ku, Yokohama 221-8686, Japan*

Received 18 June 2003; received in revised form 11 September 2003; accepted 19 November 2003

**Abstract**

An analysis of viscosity effects on the fluorescence quenching of 9,10-dicyanoanthracene (DCA) by the title hydroxylamines (**1**) and oxygen in protic polar solvents revealed the occurrence of a diffusion-limited emission quenching for both the quenchers. It was found that the viscosity dependence of the former quenching rate constant is a major factor that controls the magnitude of dependence of the sensitized oxidation efficiency at a given hydroxylamine concentration on the solvent viscosity. The interesting finding that an increase in solvent viscosity exerts only a minor effect on the limiting quantum yield for the reaction led us to conclude that the increased viscosity lowers the rates for both processes of the return electron transfer and the diffusive separation of radical ions to almost the same extent. This finding substantiates the intervention of a solvent-separated radical ion pair as a key intermediate. Based on molecular size effects on the limiting quantum yield in methanol, it was suggested that an unpaired electron generated on the hydroxylamino nitrogen is not appreciably delocalized into the aromatic rings, thus permitting strong electrostatic and hydrogen bonding interactions between the caged **1** cation radical–DCA anion radical pair and protic polar solvent molecules.


*Keywords:* Sensitized photooxidation; Hydroxylamine derivatives; Radical ion pair; Viscosity effects; Substituent effects

## 1. Introduction

Electron transfer photochemistry has continued to contribute to the development of efficient and selective transformations of organic compounds into pharmaceutically important heterocyclic compounds, as well as to the elucidation of the behavior and reactivity of a radical ion pair intermediate generated by photoinduced electron transfer [1–4]. Heretofore, much effort has been devoted to the achievement of the charge-separated state in many electron donor–acceptor model systems, which plays an essential role in constructing a highly efficient light energy-storage system [5,6]. In this regard, Marcus has made great contributions to elucidating factors that control reverse electron transfer rate in a given charge-separated state [7–10]. In a previous study we found that in the presence of an electron-accepting sensitizer and oxygen, the photoinduced electron transfer reaction of *N*,*N*-dibenzylhydroxylamine proceeds cleanly to give *N*-benzylidenebenzylamine *N*-oxide in quantitative yield and, hence, is an excellent model system for clarifying the oxidation mechanism of aliphatic hydroxylamines and related amines [11]. In addition, we discovered the Marcus 'inverted region' by controlling the ability of a sensitizer to accept electron from the hydroxylamine and also found the participation of contact and solvent-separated radical ion pairs in the primary oxidation process [12]. The question encountered in the previous study is whether back electron transfer and diffusive separation of caged radical ions proceed through a contact or a solvent-separated radical ion pair or both intermediates in the 9,10-dicyanoanthracene (DCA)-sensitized photooxidation of the model hydroxylamines in polar solvents. Systematic studies on the mechanism of acyloxy photomigration demonstrated that quantum yields for the 1,3- and 1,5-acyloxy-migrated products derived from recombination of radicals within caged contact and solvent-separated radical pairs, respectively, exhibit a different dependence on solvent viscosity [13,14]. This finding led us to explore viscosity effects on the quantum yields for formation of *N*-benzylidenebenzylamine *N*-oxide and its derivatives in order to shed much light on the question described above. Taking into account that molecular dimension may affect the rate of back electron transfer within photogenerated geminate radical ion pairs [4,15,16], we

* Corresponding author. Tel.: +81-45-481-5661; fax: +81-45-491-7915.
*E-mail address:* sakurt01@kanagawa-u.ac.jp (T. Sakurai).

1010-6030/$ – see front matter © 2004 Elsevier B.V. All rights reserved.
doi:10.1016/j.jphotochem.2003.11.008

designed and synthesized **1a–d** as model *N*,*N*-disubstituted hydroxylamines for investigating viscosity effects on DCA-sensitized photooxidation of these hydroxylamines in protic polar solvents whose viscosity was adjusted by using methanol and glycerol of comparable polarity.

## 2. Results and discussion

In a previous study we confirmed that the DCA-sensitized photooxidation of **1a** in oxygen-saturated acetonitrile or methanol proceeds cleanly to give *N*-benzylidenebenzylamine *N*-oxide (**2a**) and hydrogen peroxide without undergoing any side reactions of these products at low conversions of the starting **1a** (<20%) (Scheme 1) [11]. The irradiation of a methanol solution of **1b–d** ($(1.5–5.0) \times 10^{-3}$ mol dm$^{-3}$ for **1b**, $(2.0–10.0) \times 10^{-3}$ mol dm$^{-3}$ for **1c** and $(1.0–2.5) \times 10^{-3}$ mol dm$^{-3}$ for **1d**) under the same conditions as those for **1a** ($(2.0–10.0) \times 10^{-3}$ mol dm$^{-3}$; [DCA] $= 1.0 \times 10^{-4}$ mol dm$^{-3}$) exhibited a very similar UV absorption spectral change in which the characteristic absorption of the product was fully consistent with that of the corresponding authentic *N*-oxide (**2b–d**) prepared independently (Scheme 1). The finding that the presence of glycerol exerts no effect on the mode of this spectral change allows us to conclude that the sensitized photooxidation of the starting **1** proceeds (according to Scheme 1) to afford **2** and hydrogen peroxide quantitatively at low conversions.

In order to discuss solvent viscosity effects on DCA-sensitized oxidation processes of **1** in methanol, we propose Scheme 2 on the basis of the previous findings, where the reaction occurs by a superoxide mechanism and electron transfer from **1** to the excited singlet-state DCA forms a geminate radical ion pair intermediate. Bilski et al. reported that the sensitized photooxidation of *N*,*N*-diethylhydroxylamine gives hydrogen peroxide as one of the major products and the diethylnitroxide intermediate plays a central role in this sensitized oxidation [17]. In addition, if we take into account that the hydroxyl proton of hydroxylamines has a relatively

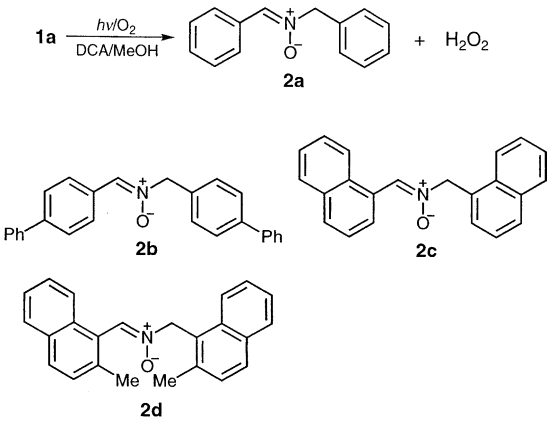


Scheme 1. Products obtained by DCA-sensitized photooxidation of **1a–d** in oxygen-saturated methanol.

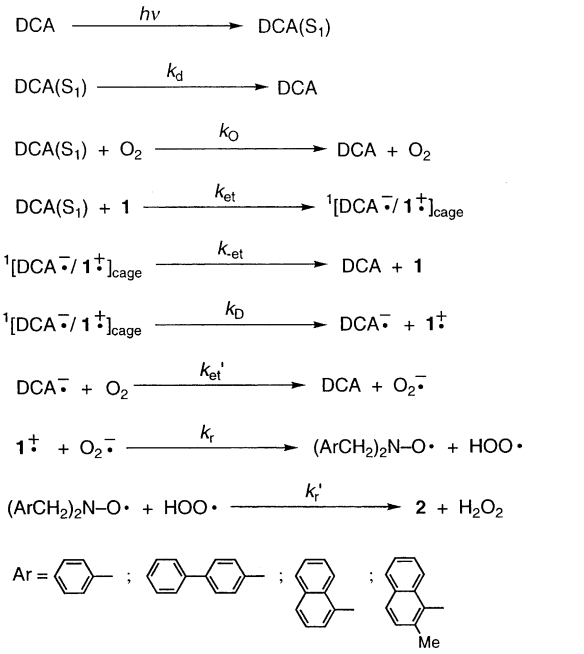


Scheme 2. Reaction mechanism proposed for the DCA-sensitized photooxidation of **1** in oxygen-saturated methanol and methanol containing glycerol.

large dissociation ability [18], the reaction of **1** cation radical with superoxide in Scheme 2 is considered to afford **1**-derived nitroxide and hydroperoxyl radical via direct proton transfer, as previously proposed. Because deactivation process of **1** cation radical and DCA anion radical by intermolecular back electron transfer is included in that of a geminate radical ion pair, $k_{-et}$ in Scheme 2 refers to the total rate constant for deactivation of this intermediate via back electron transfer.

Scheme 2 forces us to examine at first viscosity effects on the fluorescence quenching of DCA by **1** and oxygen, as well as on the fluorescence lifetime of this sensitizer. As typically shown in Fig. 1, the fluorescence of DCA was quenched by **1a** in nitrogen-saturated methanol containing 0, 25 and 50 vol.% glycerol according to the Stern–Volmer equation (Eq. (1)), where $I$ and $I_0$ are the fluorescence intensities of DCA with and without **1a–d**, respectively, $k_{et}$ is the quenching rate constant, and $\tau_S$ the fluorescence lifetime of DCA (in the absence of the quencher **1**) and was estimated to be 13.0 ns irrespective of solvent viscosity, $\eta$. Similar emission quenching behavior was

$$\frac{I_0}{I} = 1 + k_{et}\tau_S[\mathbf{1a–d}] \quad (1)$$

observed also for **1b–d** in protic polar solvents of differing viscosity. In Table 1 are collected the $k_{et}$ values evaluated from the slopes of linear Stern–Volmer plots and the emission lifetime. The data show that an increase in solvent viscosity lowers the fluorescence quenching rate for any starting hydroxylamines while the replacement of phenyl groups in **1a** by biphenylyl (**1b**) or naphthyl (**1c** and **1d**)

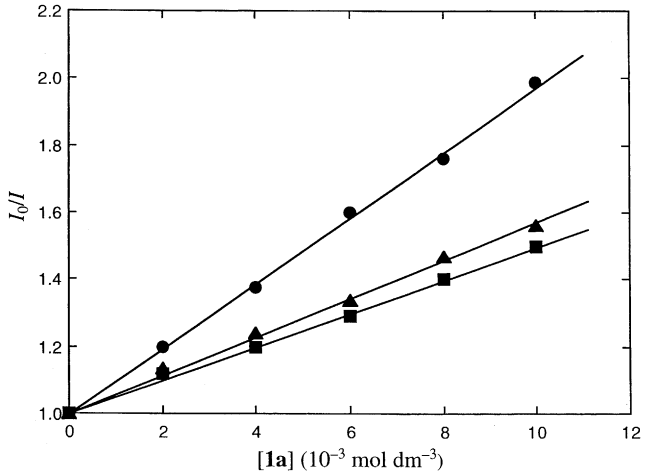


Fig. 1. Stern–Volmer plots for the fluorescence quenching of DCA ($1.0 \times 10^{-4}$ mol dm$^{-3}$) by **1a** in nitrogen-saturated methanol (●) and methanol containing 25 vol.% (▲) and 50 vol.% (■) glycerol at 24±1 °C. Excitation wavelength is 366 nm.

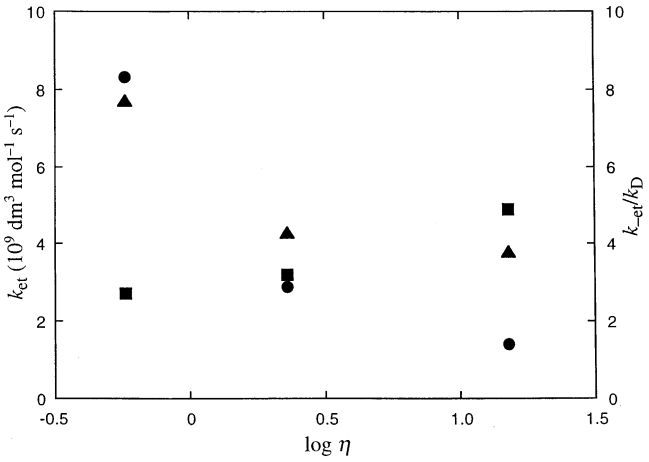


Fig. 2. Viscosity dependence of $k_{et}$ (●, ▲) and $k_{-et}/k_D$ (■) evaluated from analyses of the $\Phi_{2a}^{-1}$ vs. [**1a**]$^{-1}$ plot (●, ■) as well as of the Stern–Volmer plot for the fluorescence quenching of DCA by **1a** (▲).

increases the quenching rate constant in methanol by a factor of ca. 2. The former observation clearly indicates the occurrence of a diffusion-controlled emission quenching, as seen from Fig. 2. On the other hand, it is reasonable to assume that the fluorescence of DCA is quenched by oxygen according to the following Stern–Volmer equation (Eq. (2))

$$\frac{I(N_2)}{I(O_2)} = 1 + k_O \tau_S [O_2] \quad (2)$$

where $I(O_2)$ and $I(N_2)$ are the fluorescence intensities of DCA with and without saturated oxygen, respectively, and $k_O$ is the quenching rate constant. Thus, the emission-intensity measurements of DCA in oxygen- and nitrogen-saturated protic solvents allow us to estimate the $k_O[O_2]$ value in a given solvent (Table 1). The finding that the $k_O[O_2]$ value diminishes with increasing solvent viscosity substantiates the participation of a diffusion-controlled emission quenching process also in this case.

As already described above, the DCA-sensitized photooxidation of **1a–d** in a given solvent quantitatively affords the corresponding *N*-oxide **2**, the amount of which can be accurately determined even at appreciably low conversions of the starting **1** (<2%) according to the spectrophotometric method. Thus, an analysis of the viscosity dependence of quantum yields for formation of **2** at different concentrations of **1** is considered to give us valuable information about factors determining the sensitized oxidation efficiency in protic polar solvents. By applying the steady-state approximation to Scheme 2, we obtain Eq. (3), where $\Phi_2$ refers to the quantum yield for appearance of **2**. As typically depicted in Fig. 3, there was a good

$$\Phi_2^{-1} = \left(1 + \frac{k_{-et}}{k_D}\right)\left\{1 + \frac{k_d + k_O[O_2]}{k_{et}[\mathbf{1}]}\right\} \quad (3)$$

Table 1
Viscosity effects on the kinetic parameters ($k_d$, $k_O[O_2]$, $k_{et}$, $\Phi_{2,lim}$ and $k_{-et}/k_D$) obtained by the measurements of emission lifetime and quenching of DCA and of quantum yields for the sensitized photooxidation of **1** in a given solvent

| Hydroxylamine | Solvent | Viscosity, $\eta$ (mPa s) | $k_d$ ($10^7$ s$^{-1}$) | $k_O[O_2]$ ($10^7$ s$^{-1}$) | $k_{et}$[a] ($10^9$ dm$^3$ mol$^{-1}$ s$^{-1}$) | $k_{et}$[b] ($10^9$ dm$^3$ mol$^{-1}$ s$^{-1}$) | $\Phi_{2,lim}$ | $k_{-et}/k_D$ |
|---|---|---|---|---|---|---|---|---|
| **1a** | MeOH–glycerol (1:0, v/v) | 0.57 | 7.7 | 3.9 | 7.7 | 8.3 | 0.27 | 2.7 |
| | MeOH–glycerol (3:1, v/v) | 2.30 | 7.7 | 1.9 | 4.3 | 2.9 | 0.24 | 3.2 |
| | MeOH–glycerol (1:1, v/v) | 15.15 | 7.7 | 0.89 | 3.8 | 1.4 | 0.17 | 4.9 |
| **1b** | MeOH–glycerol (1:0, v/v) | 0.57 | 7.7 | 3.9 | 13 | 17 | 0.32 | 2.1 |
| | MeOH–glycerol (3:1, v/v) | 2.30 | 7.7 | 1.9 | 5.3 | 3.7 | 0.42 | 1.4 |
| | MeOH–glycerol (1:1, v/v) | 15.15 | 7.7 | 0.89 | 2.1 | 2.4 | 0.13 | 6.7 |
| **1c** | MeOH–glycerol (1:0, v/v) | 0.57 | 7.7 | 3.9 | 13 | 19 | 0.27 | 2.7 |
| | MeOH–glycerol (3:1, v/v) | 2.30 | 7.7 | 1.9 | 5.2 | 4.2 | 0.27 | 2.7 |
| | MeOH–glycerol (1:1, v/v) | 15.15 | 7.7 | 0.89 | 4.8 | 1.2 | 0.20 | 4.0 |
| **1d** | MeOH–glycerol (1:0, v/v) | 0.57 | 7.7 | 3.9 | 16 | 21 | 0.47 | 1.1 |
| | MeOH–glycerol (3:1, v/v) | 2.30 | 7.7 | 1.9 | 12 | 8.7 | 0.37 | 1.7 |

[a] Determined from the fluorescence quenching of DCA by **1** in a given solvent.
[b] Calculated by using $k_d$, $k_O[O_2]$ and $(k_d + k_O[O_2])/k_{et}$ in a given solvent.

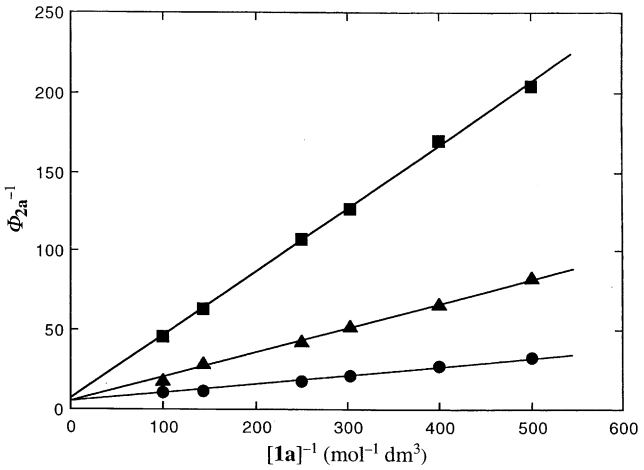


Fig. 3. Double reciprocal plots of $\Phi_{2a}^{-1}$ vs. $[1a]^{-1}$ for the DCA-sensitized photooxidation of **1a** in oxygen-saturated methanol (●) and methanol containing 25 vol.% (▲) and 50 vol.% (■) glycerol at 24 ± 2 °C.

linear relationship between the reciprocals of $\Phi_2$ ($\Phi_2^{-1}$) and **1a** concentration ($[1a]^{-1}$) in any solvents of different viscosity. The same linear relationship was observed for **1b–d**, whereas the lower solubility of **1d** made it impossible to measure quantum yields for the reaction in methanol containing 50 vol.% glycerol, as in the case of the fluorescence quenching of DCA by **1d**. From the intercept and the ratio of the slope to the intercept of linear plots obtained, we were able to estimate the limiting quantum yields, i.e., the quantum yields extrapolated to infinite concentrations of **1a–d**, for formation of **2a–d** ($\Phi_{2a-d,lim}$) and the magnitude of $(k_d + k_O[O_2])/k_{et}$, respectively. Because the $k_d$, $k_O[O_2]$ and $k_{et}$ values were already determined, it is possible to compare the $k_{et}$ values obtained by two different procedures. These are summarized in Table 1. Taking into account that the indirect method necessarily leads to a relatively large error, the two methods can be considered to give the $k_{et}$ values which are comparable to each other at any viscosity. This finding, therefore, provides strong kinetic evidence for a superoxide mechanism by which our sensitized photooxidation reactions proceed.

An inspection of Fig. 3 demonstrates that an increase in solvent viscosity makes the slope of the linear plot greater but exerts only a minor effect on the intercept. As seen from Eq. (3), the intercept and the slope are given by $(1 + k_{-et}/k_D)$ and $(1 + k_{-et}/k_D)(k_d + k_O[O_2])/k_{et}$, respectively, so that the $(k_d + k_O[O_2])/k_{et}$ value should be increased as viscosity is enhanced. In addition to the relation: $k_d > k_O[O_2]$ (Table 1), the facts that $k_d$ is little influenced by solvent viscosity and the increased viscosity lowers the quenching rate constant $k_{et}$ confirm that the slope of linear plots observed is mainly determined by the viscosity dependence of $k_{et}$. On the other hand, the starting hydroxylamines **1a–d** at their infinite concentrations can be assumed to quench the DCA fluorescence via electron transfer with 100% efficiency and, hence, Eq. (4) is derived

$$\Phi_{2,lim}^{-1} = 1 + \frac{k_{-et}}{k_D} \quad (4)$$

where $k_{-et}$ and $k_D$ are the total rate constants for return electron transfer within a geminate radical ion pair and for diffusive separation of radical ions out of this geminate ion pair intermediate, respectively. The use of Eq. (4) allows us to determine the $k_{-et}/k_D$ value (Table 1) and then to discuss viscosity effects on this relative rate for each system. Interestingly, the magnitude of the relative rate $k_{-et}/k_D$ is not very sensitive to solvent viscosity in any systems although it has a tendency to slightly increase with an increase in viscosity, as typically demonstrated in Fig. 2. This finding reveals that the increased viscosity lowers the rates for both processes of the return electron transfer and the diffusive separation of radical ions to almost the same extent, being consistent with the viscosity dependence of these two processes in a geminate radical ion pair generated by photoinduced electron transfer from tris(2,2′-bipyridine)ruthenium(II) to methylviologen [19]. It is reasonable to conclude, therefore, that the return electron transfer in a given radical ion pair and the diffusive separation of this ion pair proceed mainly from a solvent-separated radical ion pair intermediate, because solvent viscosity may exert only a small effect on the rate of back electron transfer in a contact radical ion pair. It was previously suggested that electrostatic and hydrogen bonding interactions between caged radical ions and methanol molecules are responsible for the larger limiting quantum yield in methanol than in acetonitrile [12]. It is, thus, very likely that the presence of glycerol having a higher solvation ability, as compared to that of methanol, enhances the stability of the ion pair to result in a further decrease of the back electron transfer rate [20–22]. In other words, in addition to an increase in viscosity, the larger contribution of the electrostatic and hydrogen bonding interactions described above suppresses the movements of caged radical ions (that enable their back electron transfer and diffusional separation) to almost the same extent, as observed. These considerations substantiate the intervention of a solvent-separated radical ion pair as a key intermediate in the DCA-sensitized photooxidation process of **1** in protic polar solvents.

Now we direct our attention to molecular size effects on the rate constant for back electron transfer within a solvent-separated radical ion pair intermediate generated in methanol. Since the rate constant $k_D$ can be assumed to undergo only a very small molecular size effect [4,15], the $k_{-et}/k_D$ value is a measure of the magnitude of this size effect. Through an analysis of the rates for return electron transfer within geminate radical ion pairs produced by photoinduced electron transfer from methyl-substituted benzenes, naphthalenes and biphenyls to DCA, it has been confirmed that the two-aromatic ring donors give smaller $k_{-et}$ values than the one-ring donors owing to more pronounced charge delocalization in the former [4,15]. It has also been revealed that the overall size of donor molecules is not important.

Thus, the observation that there is only a minor difference in $k_{-et}/k_D$ among **1a** (two phenyl groups), **1b** (two biphenylyl groups) and **1c** (two naphthyl groups) strongly suggests that an unpaired electron generated on the hydroxylamino nitrogen is not appreciably delocalized into the aromatic rings. This enables strong electrostatic and hydrogen bonding interactions between the caged **1** cation radical-DCA anion radical pair and protic polar solvent molecules broken into the cage. The starting **1d** bearing electron-donating methyl groups afforded smaller $k_{-et}/k_D$ value, suggesting that the **1d**-derived cation radical is stabilized by the methyl groups to some extent.

## 3. Experimental

### 3.1. Measurements

Ultraviolet (UV) absorption and fluorescence spectra were recorded on a Shimadzu UV-2200 spectrophotometer and a Shimadzu RF-5000 spectrofluorimeter, respectively. Nuclear magnetic resonance (NMR) spectra were taken with a JEOL JNM-A500 spectrometer. Chemical shifts (in ppm) were determined using tetramethylsilane as an internal standard. The fluorescence lifetime of 9,10-dicyanoanthracene was measured with a time-correlated single-photon counting apparatus (Horiba NAES-700) under the same conditions as those previously reported [11]. The viscosities of methanol and methanol containing glycerol were determined using an Ubbelohde viscometer at 25 °C. The viscosity of methanol (0.568 mPa s) was in good agreement with the literature value (0.5513 mPa s) [23]. Infrared (IR) spectra were taken with a Hitachi Model 270-30 infrared spectrometer. Elemental analyses were performed on a Perkin-Elmer 2400 series II CHNS/O analyzer.

A potassium tris(oxalato)ferrate(III) actinometer was employed to determine the quantum yields for appearance of the products **2a**–**d** at low conversions of the starting hydroxylamine **1** (<2%) [24]. A 450 W high-pressure Hg lamp was used as the light source from which 366 nm light was selected with Corning 0–52, Corning 7–60 and Toshiba IRA-25S glass filters. All of the quantum yields are an average of more than five determinations. In order to quantify the formation of **2a**–**d** spectrophotometrically, their molar absorption coefficients ($\varepsilon$) at given wavelengths were employed: $\varepsilon$ in methanol and methanol–glycerol ($dm^3\,mol^{-1}\,cm^{-1}$): $2.10 \times 10^4$ at 294 nm (**2a**), $3.69 \times 10^4$ at 317 nm (**2b**), $1.72 \times 10^4$ at 335 nm (**2c**) and $3.00 \times 10^4$ at 330 nm (**2d**).

### 3.2. Materials and solvents

*N*,*N*-Dibenzylhydroxylamine (**1a**, mp 122.0–123.0 °C; lit., 123 °C [25]) and *N*-benzylidenebenzylamine *N*-oxide (**2a**, mp 81.0–82.0 °C; lit., 81.5–83.5 °C [26]) were prepared and purified according to the previously described procedures [11]. Similar methods were applied to the preparation of **1b**–**d** and **2b**–**d**. The crude products **1b**–**d** and **2b**–**d** were purified by repeated recrystallization from EtOH–$H_2O$ to EtOAc–hexane, respectively. The physical and spectroscopic properties of these compounds are as follows.

#### 3.2.1. *N,N-Bis(4-phenylbenzyl)hydroxylamine (**1b**)*

mp 144.5–145.5 °C. IR (KBr) $\nu$: 3496 $cm^{-1}$. $^1$H NMR (500 MHz, DMSO-$d_6$) $\delta$: 3.88 (4H, s), 7.34 (2H, dd, $J$ = 7.3, 7.3 Hz), 7.45 (4H, dd, $J$ = 7.3, 8.6 Hz), 7.46 (4H, d, $J$ = 8.6 Hz), 7.61 (4H, d, $J$ = 8.6 Hz), 7.64 (4H, d, $J$ = 8.6 Hz), 7.86 (1H, s).$^{13}$C NMR (DMSO-$d_6$) $\delta$: 63.4, 126.3, 126.5, 127.2, 128.9, 129.6, 137.9, 138.7, 140.1. Analysis: calculated for $C_{26}H_{23}NO$: C, 85.45%; H, 6.34%; N, 3.83%; found: C, 85.15%; H, 6.09%; N, 3.86%.

#### 3.2.2. *N,N-Bis(1-naphthylmethyl)hydroxylamine (**1c**)*

mp 129.5–130.5 °C. IR (KBr) $\nu$: 3220 $cm^{-1}$. $^1$H NMR (500 MHz, $CDCl_3$) $\delta$: 4.22 (4H, s), 5.50 (1H, br, s), 7.30 (2H, dd, $J$ = 8.3, 9.2 Hz), 7.39 (2H, dd, $J$ = 7.3, 7.3 Hz), 7.43 (2H, dd, $J$ = 7.3, 7.3 Hz), 7.48 (2H, d, $J$ = 7.3 Hz), 7.77 (2H, d, $J$ = 7.3 Hz), 7.81 (2H, d, $J$ = 8.3 Hz), 7.87 (2H, d, $J$ = 9.2 Hz). $^{13}$C NMR ($CDCl_3$) $\delta$: 62.2, 124.6, 125.2, 125.6, 125.8, 128.39, 128.45, 128.6, 132.3, 133.1, 133.8. Analysis: calculated for $C_{22}H_{19}NO$: C, 84.31%; H, 6.11%; N, 4.47%; found: C, 83.96%; H, 6.15%; N, 4.38%.

#### 3.2.3. *N,N-Bis[1-(2-methyl)naphthylmethyl]hydroxylamine (**1d**)*

mp 189.0–190.0 °C. IR (KBr) $\nu$: 3302 $cm^{-1}$. $^1$H NMR (500 MHz, DMSO-$d_6$) $\delta$: 2.49 (6H, s), 4.32 (4H, s), 7.19 (2H, dd, $J$ = 8.2, 8.6 Hz), 7.31 (2H, dd, $J$ = 7.3, 8.2 Hz), 7.33 (2H, d, $J$ = 8.6 Hz), 7.70 (2H, d, $J$ = 8.6 Hz), 7.77 (2H, d, $J$ = 7.3 Hz), 7.77 (1H, s), 7.96 (2H, d, $J$ = 8.6 Hz). $^{13}$C NMR (DMSO-$d_6$) $\delta$: 20.2, 56.6, 124.4, 125.0, 125.4, 127.4, 127.9, 129.1, 130.9, 132.1, 133.0, 135.6. Analysis: calculated for $C_{24}H_{23}NO$: C, 84.42%; H, 6.79%; N, 4.10%; found: C, 84.38%; H, 6.66%; N, 4.08%.

#### 3.2.4. *N-(4-Phenylbenzylidene)-N-(4-phenylbenzyl)amine N-oxide (**2b**)*

mp 228.0–228.5 °C. $^1$H NMR (500 MHz, DMSO-$d_6$) $\delta$: 5.15 (2H, s), 7.37 (1H, dd, $J$ = 7.3, 7.3 Hz), 7.40 (1H, dd, $J$ = 7.3, 7.3 Hz), 7.47 (2H, dd, $J$ = 7.3, 7.9 Hz), 7.48 (2H, dd, $J$ = 7.3, 7.9 Hz), 7.60 (2H, d, $J$ = 8.5 Hz), 7.67 (2H, d, $J$ = 7.9 Hz), 7.69 (2H, d, $J$ = 8.5 Hz), 7.73 (2H, d, $J$ = 7.9 Hz), 7.76 (2H, d, $J$ = 8.5 Hz), 8.19 (1H, s), 8.33 (2H, d, $J$ = 8.5 Hz). $^{13}$C NMR (DMSO-$d_6$) $\delta$: 70.9, 127.09, 127.09, 127.2, 127.6, 127.76, 127.84, 128.86, 128.90, 129.1, 129.4, 129.7, 132.2, 134.0, 140.2, 140.5, 142.0, 143.0. Analysis: calculated for $C_{26}H_{21}NO$: C, 85.92%; H, 5.82%; N, 3.85%; found: C, 85.76%; H, 5.83%; N, 3.65%.

#### 3.2.5. *N-(1-Naphthylmethylene)-N-(1-naphthylmethyl)amine N-oxide (**2c**)*

mp 144.0–145.5 °C. $^1$H NMR (500 MHz, DMSO-$d_6$) $\delta$: 5.66 (2H, s), 7.31 (1H, dd, $J$ = 6.4, 8.4 Hz), 7.38–7.41

(2H, m), 7.47–7.58 (4H, m), 7.66 (1H, d, $J = 6.4$ Hz), 7.78 (1H, d, $J = 8.0$ Hz), 7.82 (1H, d, $J = 8.2$ Hz), 7.92 (1H, d, $J = 8.0$ Hz), 7.95 (1H, d, $J = 8.4$ Hz), 7.97 (1H, s), 8.18 (1H, d, $J = 8.2$ Hz), 9.48 (1H, dd, $J = 0.6$, 7.6 Hz). $^{13}$C NMR (DMSO-$d_6$) $\delta$: 69.7, 121.4, 123.3, 125.4, 125.5, 125.66, 125.69, 126.4, 126.7, 126.8, 127.4, 128.9, 129.0, 129.1, 129.3, 130.25, 130.29, 130.6, 130.9, 131.9, 133.4, 133.9. Analysis: calculated for $C_{22}H_{17}NO$: C, 84.86%; H, 5.50%; N, 4.50%; found: C, 84.85%; H, 5.25%; N, 4.72%.

*3.2.6. N-[1-(2-Methyl)naphthylmethylene]-N-[1-(2-methyl)naphthylmethyl]amine N-oxide (**2d**)*

mp 203.0–205.0 °C. $^1$H NMR (500 MHz, DMSO-$d_6$) $\delta$: 2.24 (1H, s), 2.27 (2H, s), 2.46 (2H, s), 2.73 (1H, s), 5.19 (0.67H, d, $J = 14.3$ Hz), 5.24 (0.67H, d, $J = 14.3$ Hz), 5.83 (0.67H, s), 8.28 (0.33H, s), 8.30 (0.67H, s), 7.15–8.45 (12H, m). $^{13}$C NMR (DMSO-$d_6$) $\delta$: 19.8, 19.9, 20.1, 20.2, 57.0, 62.1, 123.1, 123.6, 124.3, 124.5, 124.7, 125.1, 125.7, 125.8, 126.0, 126.2, 126.3, 126.6, 126.7, 127.4, 128.1, 128.3, 128.4, 128.5, 128.56, 128.59, 128.8, 128.86, 128.93, 129.1, 129.2, 129.8, 130.6, 131.22, 131.25, 131.70, 131.73, 132.09, 132.14, 132.3, 132.6, 133.5, 136.1, 136.6, 137.3, 137.5. Analysis: calculated for $C_{24}H_{21}NO$: C, 84.92%; H, 6.24%; N, 4.13%; found: C, 84.65%; H, 6.08%; N, 3.99%. These spectroscopic data clearly indicate that the *N*-oxide **2d** exists as two isomers in solution, the composition ratio of which is 2:1.

9,10-Dicyanoanthracene was purified by repeated recrystallization from toluene. Glycerol was of spectroscopic grade and used without further purification. Methanol was purified according to the standard method [21]. All other chemicals employed were obtained from commercial sources and were of the highest grade available.

## Acknowledgements

This research was partially supported by a “High-Tech Research Center Project” from the Ministry of Education, Culture, Sports, Science and Technology, Japan.

## References

[1] P.S. Mariano, J.L. Stavinoha, in: W.M. Horspool (Ed.), Synthetic Organic Photochemistry, Plenum Press, New York, 1984, pp. 145–257.
[2] G.J. Kavarnos, N.J. Turro, Chem. Rev. 86 (1986) 401.
[3] M.A. Fox, M.T. Dulay, Chem. Rev. 93 (1993) 341.
[4] I.R. Gould, S. Farid, Acc. Chem. Res. 29 (1996) 522.
[5] J.R. Norris, D. Meisel (Eds.), Photochemical Energy Conversion, Elsevier, New York, 1988.
[6] M.A. Fox, M. Chanon (Eds.), Photoinduced Electron Transfer, Elsevier, New York, 1988.
[7] R.A. Marcus, J. Chem. Phys. 24 (1956) 966.
[8] R.A. Marcus, Faraday Discuss. Chem. Soc. 29 (1960) 21.
[9] R.A. Marcus, Ann. Rev. Phys. Chem. 15 (1964) 155.
[10] R.A. Marcus, J. Chem. Phys. 43 (1965) 679.
[11] T. Sakurai, Y. Uematsu, O. Tanaka, H. Inoue, J. Chem. Soc., Perkin Trans. 2 (1992) 2163.
[12] T. Sakurai, M. Yokono, K. Komiya, Y. Masuda, H. Inoue, J. Chem. Soc., Perkin Trans. 2 (1994) 2515.
[13] T. Sakurai, H. Sukegawa, H. Inoue, Bull. Chem. Soc. Jpn. 58 (1985) 2875.
[14] T. Sakurai, K. Wada, H. Inoue, Nippon Kagaku Kaishi (1993) 728.
[15] I.R. Gould, J.E. Moser, D. Ege, S. Farid, J. Am. Chem. Soc. 110 (1988) 1991.
[16] C. Serpa, L.G. Arnaut, J. Phys. Chem. A 104 (2000) 11075.
[17] P. Bilski, A.S.W. Li, C.F. Chignell, Photochem. Photobiol. 54 (1991) 345.
[18] P. Bilski, A.G. Motten, M. Bilska, C.F. Chignell, Photochem. Photobiol. 58 (1993) 11.
[19] H.-J. Wolff, D. Bürßner, U.E. Steiner, Pure Appl. Chem. 67 (1995) 167.
[20] T. Sakurai, K. Miyoshi, M. Obitsu, H. Inoue, Ber. Bunsenges. Phys. Chem. 100 (1996) 46.
[21] K. Miyoshi, K. Kubo, T. Sakurai, H. Inoue, Nippon Kagaku Kaishi (1999) 37.
[22] K. Ozawa, K. Miyoshi, K. Kubo, T. Igarashi, T. Sakurai, Nippon Kagaku Kaishi (2000) 511.
[23] J.A. Riddick, W.B. Bunger, T.K. Sakano, Organic Solvents, Wiley, Chichester, 1986.
[24] C.G. Hatchard, C.A. Parker, Proc. Roy. Soc. Lond., Ser. A 235 (1956) 518.
[25] L.W. Jones, C.N. Sneed, J. Am. Chem. Soc. 39 (1917) 674.
[26] A.C. Cope, A.C. Haven Jr., J. Am. Chem. Soc. 72 (1950) 4896.